Effects of Chromate Treatments on Environmental Stability of Lead/Tin Alloy Joints Bonded with an Ethylene-Acrylic Acid Copolymer. I. Characterization of Chromated Surfaces and Fractured Joint Surfaces

FUMIO YAMAMOTO and SHINZO YAMAKAWA, *Ibaraki Electrical Communication Laboratory, Nippon Telegraph and Telephone Public Corporation, Tokai, Ibaraki 319-11, Japan*

Synopsis

Chromated lead, tin, and lead/tin alloy surfaces have been characterized by x-ray photoelectron spectroscopy (ESCA) and ion microanalyzer (IMA). Also the locus of failure in dry conditions of these metal joints bonded with an ethylene–acrylic acid (EAA) copolymer has been estimated from analysis of the fractured surfaces by ESCA, IMA, and scanning electron microscopy (SEM). Cathodically chromated tin and lead/tin surfaces are almost completely covered with a corrosion-protective chromium oxide film, although immersion-chromated tin and lead/tin surfaces have considerable amounts of tin and lead oxides. In chromated tin joints having a chromate film of less than 100 Å, bond failure occurs cohesively in the EAA copolymer. On the other hand, chromated tin joints having a chromate film of more than 100 Å give the failure mainly at the chromate film–tin oxide interface and partly in the tin oxide.

INTRODUCTION

In many polymer–metal bonds, the inadequate resistance to humid environments has restricted the use of the bonds.[1,2] However, the mechanisms of the environmental deterioration have not been completely elucidated.[3,4] Carboxyl-containing ethylene copolymers have some actual and many potential uses in packing, coating, and adhesive fields.[5–8] The use of ethylene–acrylic acid (EAA) copolymers[6–8] is of particular interest in metal–polyethylene composites and bimetallic laminates since EAA copolymers have relatively high adhesive bondability to both polyethylene and metals. However, the long-term exposure of EAA–metal bonds to humid environments also causes the loss in bond strength[7–10] Wargotz has showed from infrared analysis that aging of copper–EAA joints at high humidity results in the formation of a copper salt of the acid function at the interphase and also suggested that a contributing cause to the bond deterioration is the solubilization of an underlying weak layer, enhanced by the presence of hydrogen ions resulting from the carboxylate formation.

In lead–EAA bonds, the adhesion loss due to underfilm corrosion under humid environments should be more significant than in other metal bonds with EAA copolymers because moist air containing organic acid-type vapors causes serious corrosion[11] of lead. In this work, we have used lead and lead/tin alloy joints with an EAA copolymer as standard adhesive interfaces to investigate the adhesion loss due to underfilm corrosion under humid environments and investigated the

Journal of Applied Polymer Science, Vol. 25, 2479–2491 (1980)

0021-8995/80/0025-2479$01.30

effects of chromate treatments on the environmental stability. ESCA has been used extensively for determining the locus of failure or whether the bond failure is within the polymer or at the polymer–metal interface. This article describes the surface characterization of chromated lead, tin,and lead/tin alloys and the locus of failure in dry conditions. The next article in this series[12] describes the environmental stability in distilled water and the failure mechanism.

EXPERIMENTAL

Tin, lead, and lead/tin alloy sheets, 0.5 mm thick, were prepared by rolling from a lead (> 99.97%) and tin (> 99.9%). The lead/tin alloy sheets involve those of 20, 38, 50, and 62% Pb. Lead sheets were degreased in an aqueous solution of 7% CH_3COOH at 25°C for 20 sec. Tin and lead/tin alloy sheets were polished with 0.3 μm alumina in water and then degreased cathodically in an aqueous solution of 0.5% Na_2CO_3 at a voltage of 3.5 V at 30°C for 2 min. The degreased sheets were chromated at 60°C by two methods: immersion and cathodic treatments. The immersion treatment was carried out in a solution of 5 g/liter $Na_2Cr_2O_7 \cdot 2H_2O$ and 10 g/liter NaOH. The cathodic treatment was carried out in a solution of 20 g/liter $Na_2Cr_2O_7 \cdot 2H_2O$ at a current density of 5 A/dm^2. The chromated sheets were rinsed with tap water and then dried at 60°C for 24 hr.

The amount of surface tin oxide was measured by electrolytic reduction in an aqueous solution of 0.1 mole/liter NH_4Cl at a constant current density of 90 μA/cm^2 under nitrogen gas. The cathodic polarization curve of tin was measured at an increasing voltage of 50 mV/min in an aqueous solution of 0.1 mole/liter NH_4Cl. The corrosion resistance of chromated tin surface was evaluated by observation under an optical microscope after etched at 23°C for 40 sec in a corrosive solution of 100 g/liter $FeCl_3$, 20 ml/liter HCl, and 1000 ml/liter C_2H_5OH.

The thickness of chromate films on tin surface was ellipsometrically determined using a computer program of the Drude formula[13] and an optical constant of 1.3–0.3i. The ellipsometry was carried out at incident angles of 65° and 70° with a mercury arc light source of 5400 Å.

The chromated metal surfaces before bonding and the peeled surfaces of the joints were determined by ESCA. ESCA spectra were recorded on an AEI ES 200 spectrometer using Al K$\alpha_{1,2}$ radiation. Typical operating conditions were: x-ray gun, 10 kV, 20 mA; pressure in the sample chamber, 1×10^{-7} torr. The binding energies were calibrated with respect to the C 1s electron peak at 284.9 eV because of residual pump oil on the sample surface.

IMA was carried out by using a Hitachi IMA-2 spectrometer, which provided an A^+ ion beam of 4 keV and 10 mA/cm^2 at $\sim 10^{-6}$ torr. The ion beam of 0.5 mm$^\phi$ was scanned with the width of 5 mm and the depth profile was measured in the center. The sputter ratio was found to be 2–3 Å/sec.

A T-peel specimen, consisting of metal (0.5 mm), adhesive (0.2 mm), and metal (0.5 mm), was prepared by heating for 5 min with a hot press at 120°C. The adhesive used was an ethylene–acrylic acid (EAA) copolymer supplied by Union Carbide Co. (melt index 50 g/10 min, acrylic acid content 20 wt %). The T-peel strength was measured according to a method described in ASTM D1876-61T. The specimen width was 10 mm, and the crosshead speed was 100 mm/min.

RESULTS AND DISCUSSION

Chromated Tin Surfaces

Figure 1 shows the increase in chromate film thickness with cathodic treatment time, where the thickness was measured by ellipsometry. Mere immersion (treatment time of 0) produced a thickness of ~ 60 Å. Immersion treatment with an alkaline sodium dichromate solution produced a similar thickness of chromate film. The thickness increases with treatment time and levels off at ~ 300 Å.

Figure 2 shows ESCA spectra from chromated tin surfaces, and Table I summarizes the surface composition ratios in at. %, which were obtained by the use of Jørgensen's set[14] of elemental sensitivities. The tin $3d_{5/2}$ spectrum has two peaks corresponding to the metal (484.3 eV) and the oxide (486.5 eV).[15] The chromium $2p_{3/2}$ spectrum has an oxide peak (577.0 eV) having a higher binding energy than that of the metal (575.0eV).[16] With treatment time or with coverage of the tin surface with chromate film, the Sn $3d_{5/2}$ peaks decrease and the Cr $2p_{3/2}$ peak increases (Fig. 2). The immersion-chromated surface has higher remaining Sn $3d_{5/2}$ peaks and a lower increased Cr $2p_{3/2}$ peak than the cathodically chromated surface. This indicates that the former has a thinner chromate film than the latter. The metal/oxide peak ratio of Sn $3d_{5/2}$ on the cathodically chromated surface is larger than that in the untreated surface, and it increases with treatment time. This indicates that the oxide layer is etched during treatment, concurrently with formation of the chromate film.

Figure 3 shows the Cr $3p$ spectrum of the tin surface chromated cathodically for 30 sec. The Cr $3p$ spectrum shows larger chemical shifts than the Cr $2p$ spectrum, although the former is less intense than the latter.[16] Therefore, the use of the former is more useful for the composition analysis of chromated surfaces. Dickinson et al.[17] used the Cr $3p$ spectrum for the surface characterization of the chromate film deposited cathodically on a gold electrode from a chromic acid solution. According to the results,[17] the chromate film surface consists of 63% chromium (III) (44.6 eV), 11% chromium (IV–V) (46.2–46.4 eV), 26% chromium (VI) (48.0 eV), and no chromium metal (42.0 eV). All the results indicate that the cathodically chromated tin surfaces are almost completely covered with the chromate film, consisting of chromium oxides.

Figure 4 shows the cathodic polarization curves of chromated tin surfaces. The reduction peak of tin oxide is seen at −0.74 V (vs. SCE) on the untreated tin surface. The peak height decreases significantly with treatment. Since the

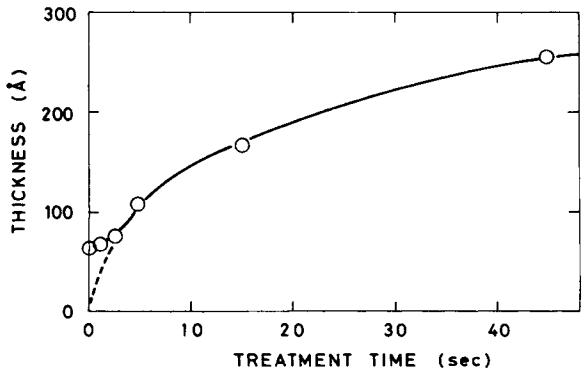

Fig. 1. Thickness of chromate film plotted as a function of chromate treatment time.

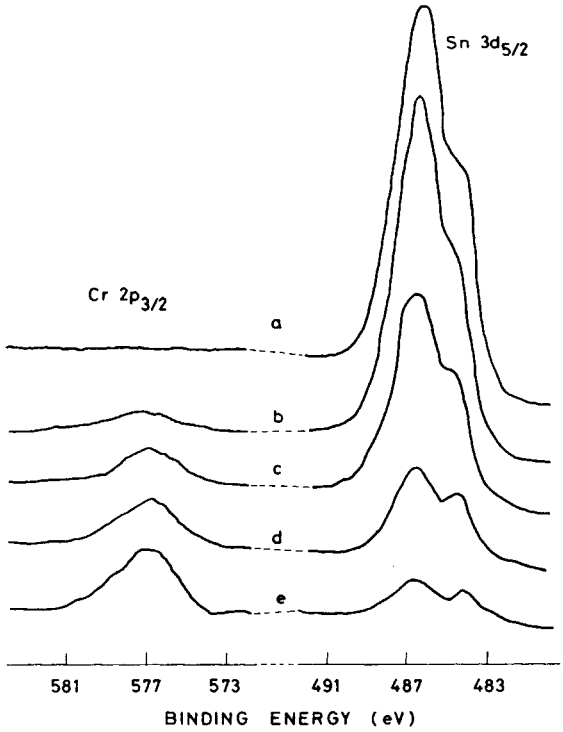

Fig. 2. ESCA spectra of chromated tin surfaces: (a) untreated; (b) immersion treated for 15 sec; (c) immersion treated for 60 sec; (d) cathodically treated for 5 sec; (e) cathodically treated for 30 sec.

decrease reflects the extent of coverage of the tin surface with chromate film, the significant decrease in the peak height of cathodically chromated surfaces indicates that the tin surface is effectively covered with the chromate film. The amount of reducible tin oxide showed a similar decrease with treatment. The amount decreased from 1.9 to 0.13 mc/cm^2 when tin was cathodically chromated.

Figure 5 shows the optical micrographs of chromated tin surfaces etched in a corrosive solution. The untreated and immersion-chromated tin surfaces shows blackish parts, which are identified as the tin corrosive surfaces (220), (200), and (211).[18] On the other hand, cathodically chromated surfaces do not give such corroded surfaces but only the corroded grain boundaries. This result also indicates that the cathodically chromated tin surfaces are covered almost completely with a protective chromate film.

TABLE I
ESCA Composition Ratio of Chromated Tin Surfaces

Surface [time (sec)]	Composition ratio (at. %)		
	O	Cr	Sn
Untreated	69.9	0	30.1
Immersion chromated (15)	74.1	4.4	21.5
Immersion chromated (60)	81.3	8.1	10.6
Cathodically chromated (5)	79.4	14.3	6.3
Cathodically chromated (30)	80.6	16.9	2.5

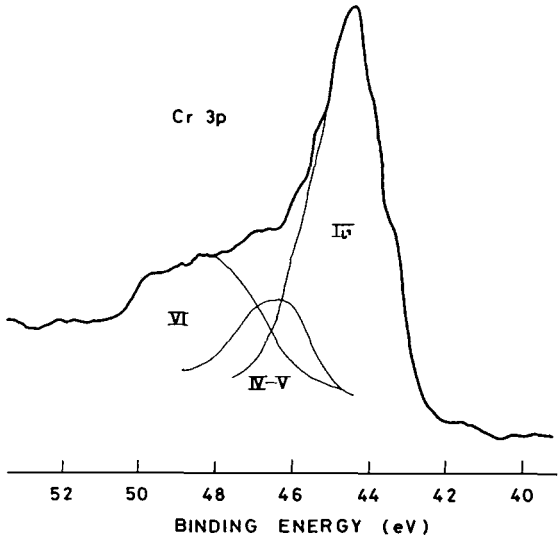

Fig. 3. ESCA 3*p* spectrum of chromium from tin surface cathodically treated for 30 sec.

Chromated Lead/Tin Alloy Surfaces

Figure 6 shows ESCA spectra of lead/tin 38/62 alloy and its cathodically chromated surfaces, and Table II shows the ESCA composition ratios in at. %, which were obtained by the use of Jørgensen's set[14] of elemental sensitivities. The ESCA spectra indicate that both lead and tin components exist both in the metallic and oxidized states; i.e., 137.0 and 139.4 eV for the Pb $4f_{7/2}$, and 484.3 and 486.5 eV for the Sn $3d_{5/2}$, respectively. The metal/oxide peak ratios of Pb

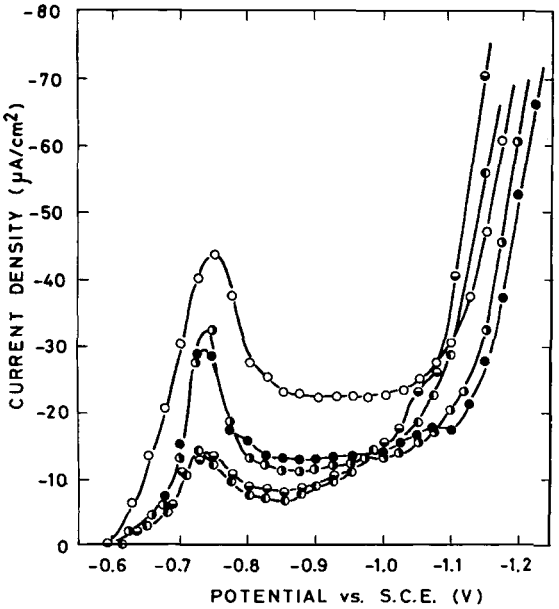

Fig. 4. Cathodic polarization curves of tin in 0.1 mole/liter NH_4Cl aqueous solution: (○) untreated; (◑) immersion treated for 15 sec; (●) immersion treated for 60 sec; (◐) cathodically treated for 5 sec; (⊖) cathodically treated for 30 sec.

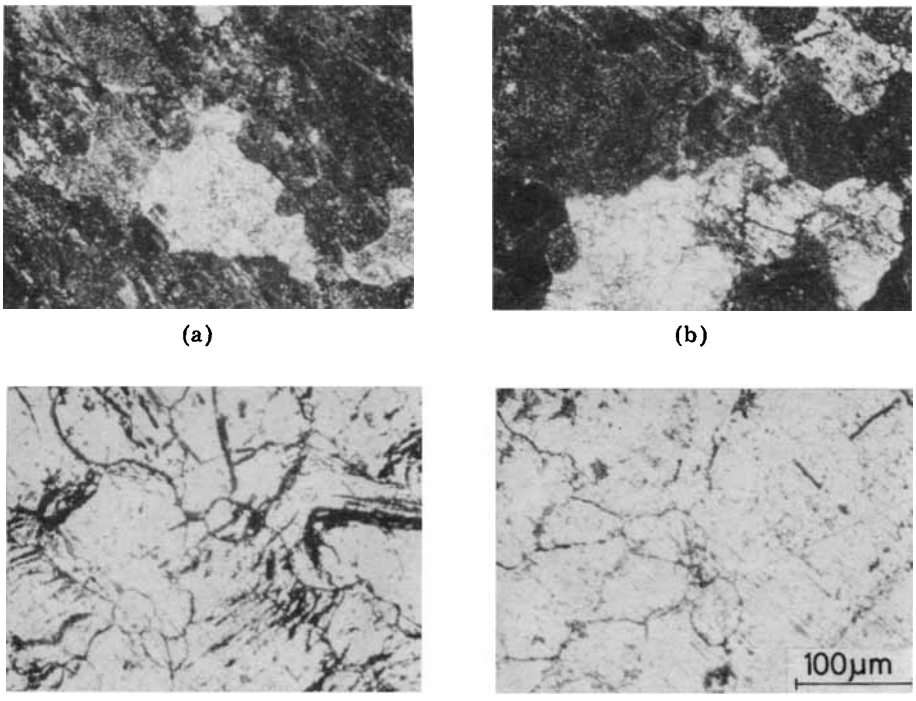

Fig. 5. Optical micrographs of corrosion-resistant tin surfaces: (a) untreated; (b) immersion treated for 60 sec; (c) cathodically treated for 5 sec; (d) cathodically treated for 30 sec.

$4f_{7/2}$ and Sn $3d_{5/2}$ indicate that both the untreated and cathodically chromated alloy surfaces are highly oxidized. The tin and lead peaks decrease significantly with treatment time and level off in 25 sec, whereas the chromium peak increases. These changes in ESCA peak heights are in good agreement with those of cathodically chromated tin surfaces.

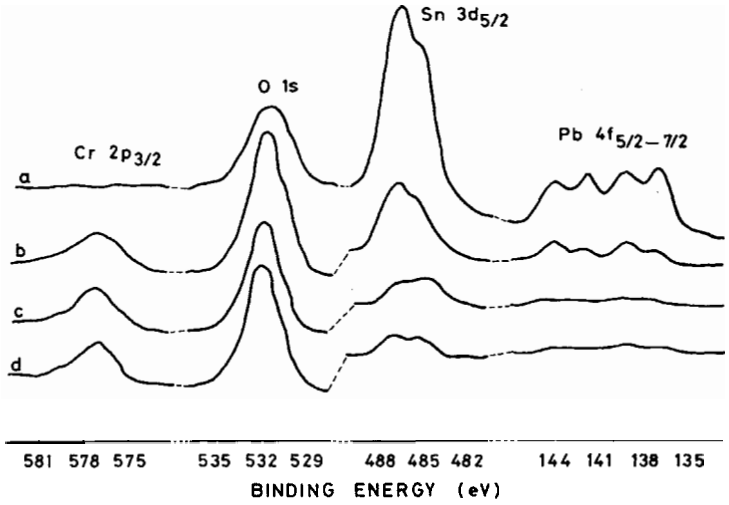

Fig. 6. ESCA spectra of cathodically chromated lead/tin alloy surfaces: (a) untreated; (b) 5 sec; (c) 25 sec; (d) 60 sec.

TABLE II
ESCA Composition Ratio of 38% Lead/Tin Alloy Surfaces

Surface [time (sec)]	Composition ratio (at. %)						
			Sn		Pb		Cr
	O	C	Metal	Oxide	Metal	Oxide	Oxide
38% lead/tin alloy	38.5	44.6	4.2	6.5	2.3	3.8	0
Cathodically chromated (5)	42.9	45.5	1.3	2.1	~0.4	0.9	7.0
Cathodically chromated (25)	42.5	43.8	0.9	0.9	~0.4	~0.4	11.1
Cathodically chromated (60)	43.9	44.7	0.9	0.9	~0.4	~0.4	8.8

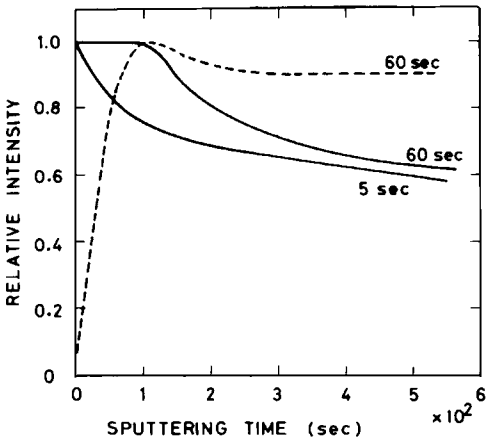

Fig. 7. Chromium and tin depth profiles of cathodically chromated lead/tin alloy surfaces: (—) ^{52}Cr; (- - -) ^{120}Sn. Figures on profiles are the treatment time (sec).

Figure 7 shows chromium and tin depth profiles by IMA analysis of cathodically chromated alloys. In the surface chromated for 60 sec, the chromium intensity decreases with sputtering time after duration of an initial maximum, whereas it decreases monotonously from the initial point in the surface chromated for 5 sec. This result shows that the chromate film thickness increases with chromate treatment time and that the surface chromated for 60 sec is completely covered with chromate film. This coincides with the above ESCA

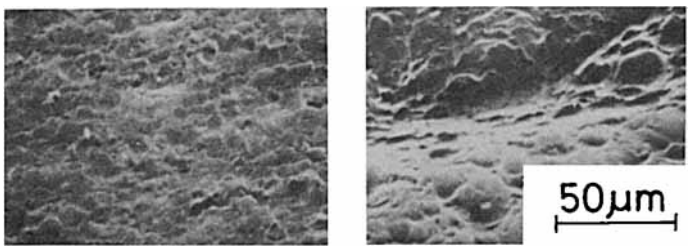

(a)

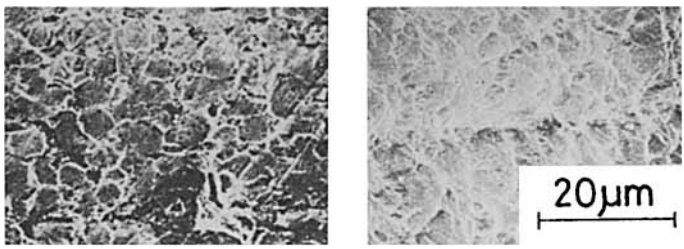

(b)

Fig. 8 Scanning electron micrographs of fractured alloy (left) and adhesive (right) surfaces of chromated alloy joints: (a) chromated to a thickness of less than 100 Å; (b) chromated to a thickness of more than 100 Å.

TABLE III
ESCA Analysis of Peeled Surfaces of Cathodically Chromated Lead/Tin Alloy Joints

Surface	Composition ratio (at. %)						
			Sn		Pb		Cr
	O	C	Metal	Oxide	Metal	Oxide	Oxide
Original alloy	38.5	44.6	4.2	6.5	2.3	3.8	0
Original alloy, chromated[a]	42.9	45.5	1.3	2.1	~0.4	0.9	7.0
Original EAA	9.6	90.4	0	0	0	0	0
Peeled alloy, lightly chromated[a]	12.1	85.7	~0.2	0.7	0.2	1.1	0.1>
Peeled EAA, lightly chromated[a]	12.6	85.9	0.1>	1.0	0.1>	~0.3	0.1>
Peeled alloy, heavily chromated[b]	30.0	57.1	2.7	7.2	0.6	1.8	0.6
Peeled EAA, heavily chromated[b]	23.9	71.7	0.1>	1.4	0.1>	~0.4	2.4

[a] Chromated to a thickness of 50+100 Å.
[b] Chromated to a thickness of ~200 Å.

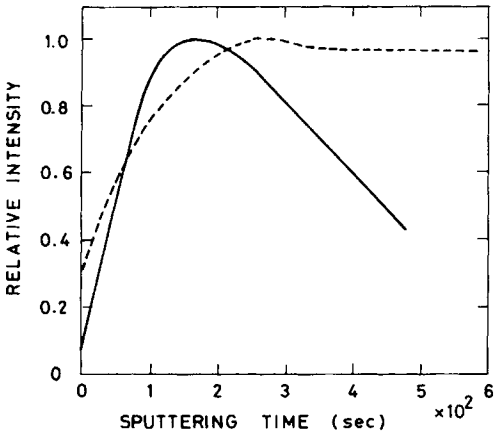

Fig. 9. Typical chromium and tin depth profiles of a peeled alloy surface: (—) ^{52}Cr; (---) ^{120}Sn.

results. The thickness is estimated to be 200–300 Å. On the other hand, the tin intensity increases gradually with sputtering time, passes through a maximum, decreases, and then becomes a constant. The maximum depth coincides with the starting point of the decrease in chromium intensity. In other words, the point corresponds to the interphase of the outer chromate layer and the inner alloy oxide layer. The appearance of the maximum point results probably from the higher sensitivity of tin oxide for IMA analysis than that of tin metal.

Locus of Failure of Dry Joints

Figure 8 shows the SEM micrographs of fractured surfaces of chromated lead/tin alloy joints peeled in dry conditions. Table III summarizes the ESCA composition ratios of the fractured surfaces. In adhesive joints of lead/tin alloy sheets cathodically chromated for a short time (e.g., 5 sec), which have probably a thin chromate film of less than 100 Å (see the next section), the SEM micrograph of the peeled adhesive surface shows significant plastic deformation of the adhesive, although that of the peeled alloy surface shows no visible transfer of the adhesive copolymer from the adhesive side to the substrate side. However,

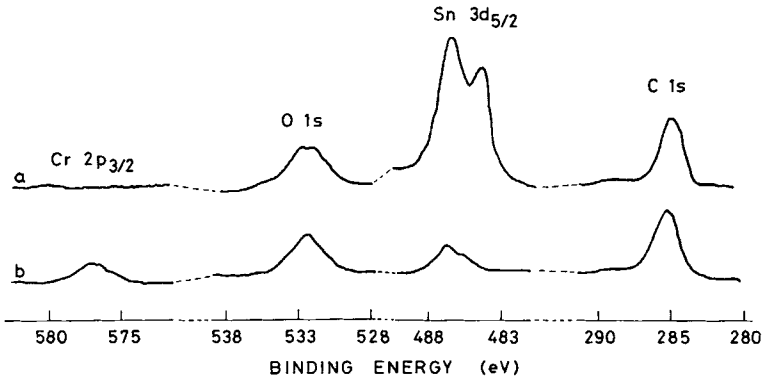

Fig. 10. Transfer of chromium from tin surface to adhesive surface: (a) peeled tin surface; (b) peeled adhesive surface.

TABLE IV
ESCA Analysis of Peeled Surfaces of Cathodically Chromated Tin Joints

Surface	Composition ratio (at. %)			
	O	C	Sn	Cr
Original tin	31.0	55.7	13.3	0
Original tin, chromated[a]	45.9	42.2	3.6	8.3
Original EAA	9.6	90.4	0	0
Peeled tin, lightly chromated[a]	9.1	90.0	0.7	~0.2
Peeled EAA, lightly chromated[a]	9.0	90.8	~0.2	0
Peeled tin, heavily chromated[b]	25.0	64.6	10.4	0
Peeled EAA, heavily chromated[b]	24.5	66.6	2.0	6.9

[a] Chromated to a thickness of 50+100 Å.
[b] Chromated to a thickness of ~200 Å.

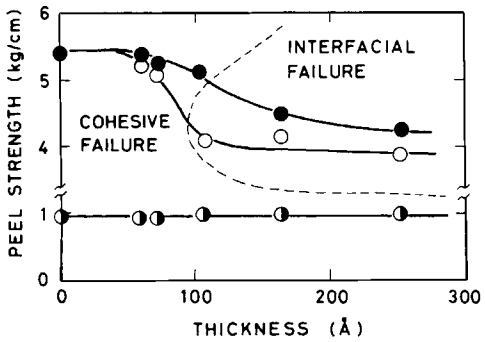

Fig. 11. Peel strength plotted as a function of the thickness of chromate film. Peel temperature: (●) 40°C; (○) 20°C; (◑) 5°C.

ESCA observations indicate that both the peeled alloy and EAA surfaces show an overall ESCA spectrum similar to that of the original adhesive surface, although there is a slight transfer of tin and lead components from the substrate side to the adhesive side (Table III). These results indicate that the bond failure occurs mainly in the adhesive near the interface. Figure 9 shows typical chromium and tin depth profiles by IMA analysis of the peeled alloy surface. The chromium intensity increases, passes through a maximum, and then decreases with sputtering time, whereas in the case of the original alloy surface the chromium intensity decreases monotonously with sputtering time (Fig. 7). The initial increase in chromium intensity of the peeled surface probably indicates that the peeled surface is covered with the adhesive and thus that the failure occurs cohesively in the adhesive. On the other hand, the fractured surfaces of lead/tin alloy joints cathodically chromated for a long time (e.g., more than 25 sec), which have probably a thick chromate film of more than 100 Å (see the next section), give a fractured topography (Fig. 8) different from that of the fractured alloy joints chromated for 5 sec. The ESCA composition ratio (Table III) shows a significant appearance of Cr and Sn oxide peaks on the adhesive side and a decrease in Cr peaks on the alloy side. This result indicates that the failure occurs between the chromate film and the underlying alloy.

Table IV gives the ESCA composition ratios of fractured surfaces of chromated tin joints peeled in dry conditions. In chromated tin joints having a chromate film of less than 100 Å, the peeled tin and EAA surfaces give identical ESCA spectra, which is similar to that of the original EAA. This result indicates that the failure occurs cohesively in the adhesive. On the other hand, chromated tin joints having a chromate film of more than 100 Å give the failure at the chromate film–tin oxide interface and in the tin oxide, which is the same as in alloy joints heavily chromated. The peeled tin surface has no Cr 2*p* peak, and the peeled adhesive surface has a chromium peak (Fig. 10). This indicates the transfer of the chromate film from the tin side to the adhesive side.

In chromated lead joints, the fracture occurred also at the chromate film–lead oxide interface or in the lead oxide regardless of the chromate film thickness. ESCA analysis of fractured lead joints showed the transfer of the chromate film from the lead side to the adhesive side. The ESCA spectra showed a significant appearance of Cr and Pb peaks on the adhesive side and a decrease in Cr peak on the lead side.

Relationship between Dry Peel Strength and Chromate Film Thickness

Figure 11 shows dry peel strength versus chromate film thickness of cathodically chromated tin sheets. At a peeling temperature of 20°C, the dry peel strength decreases rapidly at 80–100 Å of chromate film thickness. At a peeling temperature of 40°C, it decreases at similar thickness. Also the locus of failure, which is determined by ESCA analysis of peeled surfaces, is shown in Figure 11. At peeling temperatures at 20 and 40°C, the locus of failure changes from cohesive failure in the adhesive layer to interfacial failure at chromate film–tin oxide with chromate film thickness. The transition zone coincides approximately with the transition zone in dry peel strength. At a peeling temperature of 5°C, failure occurs in the adhesive layer, independent of chromate film thickness. Cathodically chromated lead/tin alloy joints gave a transition zone (in dry peel strength and in locus of failure) similar to that of chromated tin joints, although the accurate thickness of chromate film could not be measured.

References

1. D. J. Falconer, N. C. MacDonald, and P. Walker, *Chem. Ind. London,* 1230 (1964).
2. R. F. Wegman, *J. Appl. Polym. Sci. Appl. Polym. Symp.*, **19,** 385 (1972).
3. R. A. Gledhill and A. J. Kinloch, *J. Adhes.*, **6,** 315 (1974).
4. N. J. Delollis and O. Montoya, *J. Appl. Polym. Sci.*, **11,** 983 (1967).
5. J. W. Sawyer and R. E. Stuart, *Mod. Plast.*, **44,** 125 (1965).
6. G. E. Clock, G. A. Klumb, and R. C. Mildner, *12th International Wire and Cable Symposium,* Asbury Park, NY, 1963.
7. H. G. Frank, M. C. McGaugh, and W. E. Ropp, *17th International Wire and Cable Symposium,* Atlantic City, NJ, 1968.
8. B. Wargotz, *J. Appl. Polym. Sci.*, **13,** 1965 (1969).
9. W. H. Smarook and S. Bonotto, *Polym. Eng. Sci.*, **8,** 41 (1968).
10. B. Wargotz, *J. Appl. Polym, Sci.*, **12,** 1873 (1968).
11. H. H. Uhlig, *Corrosion Handbook,* Wiley, New York, 1948.
12. F. Yamamoto, S. Yamakawa, and M. Wagatsuma, *J. Appl. Polym. Sci.*, to appear.
13. M. Born and E. Wolf, *Principles of Optics,* Pergamon, New York, 1964.
14. H. Berthou and C. K. Jørgensen, *Anal. Chem.*, **47,** 482 (1975).
15. R. O. Ansell, T. Dickinson, A. F. Povey, and P. M. A. Sherwood, *J. Electrochem. Soc.*, **124,** 1360 (1977).
16. K. Siegbahn, C. Nordling, A. Fahlman, R. Nordberg, K. Hamrin, J. Hedman, G. Johansson, T. Bergmark, S.-E. Karlsson, I. Lindgren, and B. Lindberg, *ESCA-Atomic, Molecular, and Solid State Structure Studies by Means of Electron Spectroscopy,* Almqvist and Wiksells, Uppsala, 1967.
17. T. Dickinson, A. F. Povey, and P. M. A. Sherwood, *J. Chem. Soc. Faraday Trans. 1,* **72,** 686 (1976).
18. O. Yanagi, H. Nakaide, J. Tsujimoto, and K. Yoshida, *Tetsu To Hagane,* **54,** 250 (1968).

Received November 30, 1979
Accepted January 29, 1980